

# Absolute Magnitude Calibration for the W UMa-type Systems Based on HIPPARCOS Data<sup>1</sup>

SLAVEK M. RUCINSKI<sup>2</sup>

Electronic-mail: *rucinski@cfht.hawaii.edu*

Canada – France – Hawaii Telescope Co.

P.O.Box 1597, Kamuela, HI 96743

and

HILMAR W. DUERBECK<sup>3</sup>

Electronic-mail: *hilmar@cygnus.uni-muenster.de*

Space Telescope Science Institute, Baltimore, MD 21218

September 16, 2018

## ABSTRACT

Hipparcos parallax data for 40 contact binary stars of the W UMa-type (with  $\epsilon M_V < 0.5$ ) are used to derive a new,  $(B - V)$ -based absolute-magnitude calibration of the form  $M_V = M_V(\log P, B - V)$ . The calibration covers the ranges  $0.26 < (B - V)_0 < 1.14$ ,  $0.24 < P < 1.15$  day, and  $1.4 < M_V < 6.1$ ; it is based on a solution weighted by relative errors in the parallaxes (2.7% to 24%). Previous calibrations have not been based on such a wide period and color space, and while they have been able to predict  $M_V$  with sufficient accuracy for systems closely following the well-known period-color relation, the new calibration should be able to give also good predictions for more exotic “outlying” contact binary systems. The main limitations of this calibration are the inadequate quality of the ground-based photometric data, and the restriction to the  $(B - V)$  index, which is more sensitive to metallicity effects than the  $(V - I)$  index; metallicities are, however, basically unknown for the local W UMa-type systems.

## 1. INTRODUCTION

Contact binary stars of the W UMa-type are – externally – simple structures. They are single objects with two mass centers and surfaces described by common equipotentials so that fewer parameters are needed to describe them than is the case for detached binaries: In place of two radii, one value of potential is needed, and in place of two surface temperatures, apparently one for the common surface suffices (Rucinski 1985, Rucinski 1993). The poorly understood

---

<sup>1</sup>Based on data from the ESA Hipparcos astrometry satellite

<sup>2</sup>Affiliated with York University and University of Toronto, Canada

<sup>3</sup>Affiliated with Münster University, Germany. Permanent address: PF 1268, 54543 Daun, Germany.

complexity of their internal structure is hidden from our view. The external simplicity and the observational property of the W UMa-type systems to appear close to the main sequence were the underlying reasons for establishing an absolute-magnitude calibration (Rucinski 1994 = CAL1) in terms of two observational quantities, the orbital period  $P$  and an intrinsic color, e.g.  $(B - V)$  or  $(V - I)$ . Both quantities are correlated through the combined effects of similar geometry, Kepler’s third law and main-sequence relationships, although the correlation is not perfect because of the evolutionary spread in sizes within the main sequence.

The existence of a period – color – luminosity relation is somewhat reminiscent of that for pulsating stars. This should not be surprising if one realizes that the orbital periods for similar contact structures are in a simple relation to dynamical (or free-fall) time scales and that the radiating areas simply scale with the length of the period. A calibration of the form  $M_V = a_P \log P + a_C C + const$  (where  $C$  is for any color index) can be also considered as an attempt to shift the stress from the color-derived temperature dependence of the normal main sequence (which presents operational difficulties, as it is affected by interstellar reddening) to a period dependence controlled by Kepler’s third law. For the absolute magnitude calibration and derivation, the period can be considered essentially error-free, because it can be precisely determined by studying accumulated deviations of times of minimum light from a given ephemeris.

As explained in CAL1, no mass-luminosity relation is involved in the calibration, just the simple geometrical relations. The most important omission consists of the neglect of the mass-ratio ( $q$ ) term. The mass-ratio for newly discovered or faint systems is usually unknown as its determination requires spectroscopic observations at large telescopes, which are difficult to obtain for these typically faint and very short-period systems. Fortunately, the  $q$ -term possibly correlates with, or can be absorbed by, the two other terms. The other limitation of any luminosity calibration for contact binaries is that it is likely affected by the presence of spots on such very active stars. Therefore, the calibration applies to a somewhat poorly defined mean maximum brightness, where the averaging is over a spot-induced variability of poorly known temporal characteristics.

The first calibration (CAL1) was based on 18 systems, mostly members of high galactic-latitude open clusters (to avoid Milky Way interlopers in more typical open clusters), and of visual binaries, as well as on 3 nearby systems with known trigonometric parallaxes, 44i Boo B, VW Cep and  $\epsilon$  CrA. Even for these three systems, the data were somewhat uncertain: The color of 44i Boo B had not been measured with any degree of accuracy due to the light of the close visual companion, and large discrepancies existed between published parallax values for  $\epsilon$  CrA. From the beginning, there was a need for reliable trigonometric parallaxes for a large number of systems.

CAL1 concentrated on the  $M_V = M_V(\log P, B - V)$  relation. Further work related to an approximate evaluation of the metal abundance effects, based on systems in very metal-poor clusters (Rucinski 1995 = CAL2), and to a calibration of the relation in the form  $M_I = M_I(\log P, V - I)$ , to study the galactic distribution of systems discovered in the OGLE microlensing search (Rucinski 1997a = CAL3). In summary, the established relations were:

$$M_V = -2.38 \log P + 4.26 (B - V)_0 + 0.28 - 0.3 [\text{Fe}/\text{H}] \quad (1)$$

$$M_V = -4.43 \log P + 3.63 (V - I)_0 - 0.31 - 0.12 [\text{Fe}/\text{H}] \quad (2)$$

$$M_I = -4.6 \log P + 2.3 (V - I)_0 - 0.2 - 0.12 [\text{Fe}/\text{H}] \quad (3)$$

where the first two equations combine the results of CAL1 and CAL2, while the third combines the results of CAL2 and CAL3. The colors in Eqs. 2 and 3 are de-reddened and the  $(V - I)$  color is measured in the Kron – Cousins system. The  $(V - I)$ -based calibrations (Eqs. 2 and 3) must be considered preliminary because of the lack of directly observed colors. Due to strong inter-parametric correlations, the coefficients in the relations have very large and highly non-Gaussian errors (see CAL1 and below, Section 3). However, the absolute magnitudes can be predicted quite accurately. As was illustrated through Monte Carlo simulations, the preliminary  $M_I$  calibration (Eq. 3) could predict the absolute magnitudes to one-sigma (68.3% confidence) level of  $\pm 0.25$  magnitude and to two-sigma (95.4% confidence) level of  $\pm 0.5$  magnitude (see Figure 3 in Rucinski (1996)). At first, the period range was only  $0.27 < P < 0.59$  day, but was slightly extended to 0.63 day in CAL3.

The extant versions of the luminosity calibration have been used by several authors, mostly for consistency checks on the membership of individual newly discovered systems in various clusters (Edmonds et al. 1996, Kaluzny et al. 1996a, Kaluzny et al. 1996b, Mazur et al. 1995, Rubinstein and Bailyn 1996, and Yan and Mateo 1994). A somewhat more ambitious application was its use for distance *determinations* within the “pencil-beam” search volume of the micro-lensing project OGLE (CAL3).

Although the predictive power for individual cases is relatively low (conservatively estimated to be more accurate than 0.5 magnitude, taking into account the possibility of systematic errors), the various forms of the the calibration have a definite potential. Of particular importance is the high frequency of occurrence of the contact binaries: Disregarding the difference in population characteristics, the contact binaries are some 24,000 times more common than RR Lyr stars (CAL3) in the solar neighborhood. Thus, one can imagine their application to detailed galactic structure studies, in place or in addition to those based on RR Lyr stars. In addition, an extension of the calibration towards early-type contact systems may enhance their usefulness for more distant stellar systems. The calibrations may be also useful in obtaining a better estimate of the spatial density of contact systems. The apparent density derived from the OGLE sample (CAL3) of about one such system per 250 – 300 main sequence stars of similar spectral types (F–K) is about 3 to 4 times higher than the density estimated from a sample of systems in the solar neighborhood (Duerbeck 1984). The discrepancy may be due to incompleteness of the contact binary sample below the brightness level of about  $V = 8$ . The complete sample of the F–K stars in the Hipparcos Input Catalogue (Turon et al. 1994) contains 128, 497, 1620 and 4561 stars of luminosity classes IV and V within the range of occurrence of the W UMa-type systems,  $0.4 < (B - V) < 1.2$  to magnitude limits  $V = 5, 6, 7, 8$ . To the same brightness limits, there are 3, 3, 6, and 14 contact binaries giving the inverse relative frequencies 43, 166, 270, 326. Thus, the frequency derived from the OGLE data is approximately confirmed, but with a large statistical uncertainty and with a trend indicating that discovery selection effects become progressively stronger for fainter systems. Once a larger sample of such faint (i.e. not accessible to direct parallax measurements) contact systems is identified, the calibration can be used to define a volume-limited subsample for an unbiased local density estimate.

Parallax data from the HIPPARCOS satellite (ESA 1997) have already been used to derive a new absolute-magnitude calibration for the W UMa-type systems (Rucinski and Duerbeck 1997 = CAL4). The main motivation was the obvious need of having a solid check on the previous calibrations which had been based on inhomogeneous data from various sources. A sample defined by the errors in  $M_V$  smaller than 0.25 magnitude ( $\epsilon M_V = 2.17 \frac{\epsilon \pi}{\pi} < 0.25$ ) consisted of 20 systems, but the system with the largest and most precisely measured parallax, 44i Boo B, still does not have a reliably measured color and had to be omitted. Only 2 systems were common to CAL1 and CAL4. The calibration directly comparable to CAL1 is CAL4a:

$$M_V = -4.30 \log P + 3.28 (B - V)_0 + 0.04 \quad (4)$$

CAL4a turned out to show a small standard error ( $\sigma = 0.17$ ) and, despite its somewhat differing coefficients from those of CAL1, to give encouragingly similar predictions on  $M_V$  as compared to the previous calibrations. Monte Carlo simulations showed that, as far as random errors are considered, absolute magnitudes of contact binaries can be predicted with an accuracy of about 0.1 magnitude, which is surprisingly good in view of the omission of the mass-ratio term and of the possibility of star spots. However, deviations of individual systems from the “fundamental plane” of the calibration indicated the possibility of systematic rather than random errors, and the problem of the applicability of the calibration over wider ranges of periods and colors remained. CAL4 was established within the period range  $0.27 < P < 0.65$  day, with most calibrating systems clustering around the main period–color relationship. The experimental addition of the long-period, red system V371 Cep (V5 in NGC 188) led to very different calibration coefficients. Since the two quantities of the calibration, period and color, are strongly (but not perfectly) correlated, the calibration is extremely sensitive to the inclusion of severely spotted or non-contact systems mimicking genuine W UMa-type systems. Realizing these limitations of CAL4, we consider in the present paper a larger sample, comprising also systems with poorer parallax data, with a hope that such a sample would cover a wider range of periods and colors, and thus lead to better averaging of individual peculiarities than in the case of the 19 systems used to establish CAL4.

## 2. Hipparcos and auxiliary data

Our present sample consists of 40 systems with parallax errors implying uncertainties  $\epsilon M_V < 0.5$  magnitude. Most systems are well-known, bright W UMa-type binaries. While details on the adopted photometric data for the sample systems are given in the next section and in the extensive Appendix, several systems included in or excluded from the sample require a special mention:

- 44i Boo The color data for the contact binary which is the fainter component (B) of a close visual system are too uncertain to warrant its inclusion in the sample. 44i Boo B is the nearest contact binary with a parallax of  $78.4 \pm 1.0$  mas (milli-arcsec).
- BW Dra We included this system although the relatively uncertain parallax data ( $15.3 \pm 5.2$  mas) would formally exclude it from consideration. This system forms a visual binary with

another contact system, BV Dra. The better-quality parallax of BV Dra was assigned to BW Dra, too.

AP Dor The poorly known contact binary HD 33474 was included in the sample although only a fragmentary light curve and a coarse estimate of the period existed until now (Eggen 1980). The value of the period has been taken from the Hipparcos Catalogue (ESA 1997) where it is classified as a W UMa or possibly a RR Lyrae star. However, Eggen (1980) argued convincingly that AP Dor is a contact binary system. Its absolute magnitude also contradicts the RR Lyrae classification.

BV Eri This binary was initially included in the list of contact binaries to be studied with Hipparcos (HIC 18080), but it has been excluded from our present study since the photometric analysis of Baade et al. (1983) has shown that it is a close detached binary.

UZ Oct This contact system has period slightly longer than one day and formally does not belong to the class of W UMa-type systems. We included it in our calibration. It contributes little to the final determination, but its deviation from the calibration established for short-period systems may give us indications of the expected trends for long-period systems.

ER Ori According to the photometric and spectroscopic analysis, ER Ori should have a trigonometric parallax between 5 and 7 mas, which would probably have lead to the inclusion into our sample. The Hipparcos parallax is, however,  $-6.8 \pm 1.4$  mas. Since ER Ori is a triple system with a third component at a distance of  $0''.1$ , found by speckle observations (Goeking et al. 1994), it is likely that the orbital motion around the common center of mass has resulted in an unrealistic parallax value.

In addition to the parallaxes and the periods, the input data for the calibration consist of the observed maximum magnitudes in  $V$ , the  $(B - V)$  colors at maximum brightness, and the reddening values  $E(B - V)$ . No measured values of  $(V - I)$  were available for most systems, thus no separate  $M_V = M_V(\log P, V - I)$  calibration was attempted (in most cases, the  $(V - I)$  data listed in the final Hipparcos Catalogue have not been measured, but were derived from  $(B - V)$ ). This color index has become a standard one in CCD-based studies of stellar clusters and micro-lensing searches, and it is unfortunate that we presently do not have a good database to carry out a calibration.

The  $V$  magnitude and  $(B - V)$  color index at maximum light were usually taken from the literature, but sometimes had to be inferred from Hipparcos magnitudes or from Strömgen photometry. Details on all systems are given in the Appendix to permit a quality assessment in each case. The adopted values of the data used to establish the new calibration are listed in Table 1. It should be stressed that some of these input data have gone through a much more careful scrutiny and thus supersede those adopted in CAL4. Although our main goal was to establish reliable values of the magnitudes and colors at light maxima, both Table 1 and the Appendix update and extend a very useful compilation of parameters of contact systems by Maceroni and Van't Veer (1996), which focussed on contact systems with modern photometric solutions. Our Table includes 14 systems not listed by them – in most cases because no detailed analysis has been carried out until now.

As indicated, the available  $V_{\max}$  data for some systems were poorly known or considered not trustworthy. In such cases, we gave a higher weight to independent estimates of  $V_{\max}$ , based on the Hipparcos data for the upper 5% of the brightness (the 95-percentile levels),  $Hp_{\max}$ . Since the  $Hp$  photometric system slightly differs from  $V$ , a transformation to  $V$  magnitudes was necessary. In CAL4, we used a  $Hp$  to  $V$  transformation involving a small  $(V - I)$ -term which was estimated from the adopted  $(B - V)$  via the color – color calibrations of Bessell (1979). This two-step process has been simplified here by considering differences  $Hp - V$  directly as a function of  $(B - V)$ . Reliable values of  $Hp - V$  at maximum light for 30 of our systems were used to establish two- and one-parameter relationships,  $Hp - V = 0.17(B - V) + 0.03$  and  $Hp - V = 0.22(B - V)$ . We adopted the latter, noting that the intercept should be zero by definition, but that in the present case it may be non-zero because of the averaging at the 95-percentile level in  $Hp$ .

If no  $(B - V)$  index was available, it could sometimes be calculated from a measured  $(b - y)$  index, using relations established by Bessell (1979). Some  $(B - V)$  indices were taken from an unpublished photometric survey of southern contact binaries (Duerbeck 1997). In all instances, the data were compared with the mean data from the Tycho experiment tabulated in the Hipparcos Catalogue.

The reddening  $E(B - V)$ , although a relatively small quantity for the nearby systems considered here, can affect the calibration in a systematic way. It tended to be over-estimated in previous studies (Rucinski and Kaluzny 1981, Rucinski 1983) through the use of general distance and galactic-latitude scaling laws, which may be invalid for small distances. In fact, the mean value of the extinction of  $A_V = 1.8$  mag/kpc (Whittet 1992) applies only to situations of good averaging of many individual interstellar clouds at large distances. For moderate distances below 100 pc, and well within the galactic disk, the interstellar medium shows strong inhomogeneities, with some directions almost devoid of any absorption. The novel approach, adopted in CAL4 and in the present paper, uses values of neutral hydrogen column density,  $N_{\text{HI}}$ , to estimate  $E(B - V)$ . A large database of determinations for  $N_{\text{HI}}$  is available as an Internet hydrogen column density search tool from the Center for Extreme Ultraviolet Astrophysics in Berkeley, California<sup>4</sup>; it is based on the data in Fruscione et al. (1994). On the basis of the studies by Bohlin et al. (1978) and Tinbergen (1982), the adopted relation between  $E(B - V)$  and  $N_{\text{HI}}$  ( $\text{cm}^{-2}$ ) was:  $E(B - V) \simeq 1.7 \times 10^{-22} N_{\text{HI}}$ . A newer study, based on X-ray data (Predehl and Schmitt 1995), gives an almost identical relation with the coefficient of  $1.8 \times 10^{-22}$ , a difference which can be entirely neglected for the small values of  $E(B - V)$  encountered in here. The values of  $E(B - V)$  in Table 1 derived in the above way carry uncertainties of about 0.01 – 0.02 magnitude. On the average, they are much smaller than previously assumed for the field W UMa systems, but remain uncertain due to interpolation of the values of  $N_{\text{HI}}$  over an irregular grid of stars, with relatively large spacings in angular separation and distance.

The absolute magnitudes have been derived from  $M_V = V + 5 \log \pi - 3.1 E(B - V) - 10$ , where the parallax  $\pi$  is in milli-arcsec units ( $0''.001$ ), and the observed magnitude at maximum light is in the Johnson  $V$ -band.

---

<sup>4</sup>[http://www.cea.berkeley.edu/~science/html/sci\\_archive\\_tools\\_tools.html](http://www.cea.berkeley.edu/~science/html/sci_archive_tools_tools.html).

### 3. The new absolute-magnitude calibration

The color – absolute-magnitude diagram for the systems used in this paper is shown in Figure 1. Note the vertical spread of the points, which is mostly due to the evolution of some systems away from the main sequence and to un-accounted mass-ratio differences. Without this spread, the calibration could be simplified to just one independent variable. The period – color relation is shown in Figure 2. In these and the following figures, filled circles mark the systems with better parallax data ( $\epsilon M_V < 0.25$ ) whereas open circles mark the systems with larger relative errors in the parallaxes ( $0.25 < \epsilon M_V < 0.5$ ). There are almost exactly the same numbers of systems in each of these categories.

The combined 3-dimensional period – color – luminosity relation is shown in Figure 3. The planar fit corresponds to the calibration

$$M_V = a_{P(BV)} \log P + a_{BV} (B - V)_0 + a_{0(BV)}, \quad (5)$$

whose coefficients are listed in Table 2. The deviations from the fit are shown in Figure 4. As in the previous cases, the coefficients in Eq. 5 have errors which are very large and very strongly non-Gaussian. In CAL1 and in the following studies, the errors were estimated with a technique of “bootstrap re-sampling”, which utilizes a large number of solutions based on the observational data re-arranged randomly into several data sets of the same size by a random (and repetitious) selection of points. This technique permits to evaluate realistic errors for cases of their entirely unknown distributions. The application to our data is illustrated in Figure 5 which gives the spread in the coefficients obtained from 10,000 bootstrap re-sampling solutions. The one-sigma ranges in the diagrams can be identified with the extent of contours containing 68.3% of all cases. The essential statistics for the bootstrap re-sampling results is given in Table 2. Note that the median and average values of the coefficients are closer than in the previous calibrations, indicating a better overall stability of the current solution. Since this calibration is based on a larger sample than all previous ones, Figure 5 no longer shows multiple “islands” of the solutions which indicated that the previous versions of the calibration were sensitive to the inclusion or rejection of individual systems.

The relatively large uncertainties in the coefficients do not signify that the predicted values of absolute magnitudes are equally uncertain, as inter-parametric correlations result in cancelation of the contributing uncertainties. To determine uncertainties in the predicted absolute magnitudes, a Monte Carlo experiment was carried out. This experiment is based on the availability of the 10,000 bootstrap solutions which were used for evaluation of the coefficient errors, as described above. We added one more level of randomization here by considering 100 random values of  $(B - V)$  for each value of the period between 0.2 and 1.0 days in steps of 0.01 day. This way, *for each step in the period*,  $10^6$  random combinations of the colors and coefficients were used. Whereas the distribution of the coefficients had been given by the bootstrap re-sampling experiments, the distribution of the colors was assumed flat within period-dependent ranges. These ranges increased linearly in width from  $\Delta(B - V) = 0.3$  at the period of 0.2 day to  $\Delta(B - V) = 0.6$  at the period of one day. The widening was meant to represent the observed trend in the period – color relation, with a much larger spread in colors for long-period system. This spread is usually interpreted as due to evolutionary effects which are more pronounced for long-period systems. The blue edges

of the respective color ranges were placed at the observed blue, short-period envelope (BSPE) of the period – color distribution. The existence and importance of the BSPE was discussed in CAL3 where an approximate fitting formula was determined:  $(V - I)_{BSP} = 0.053 P^{-2.1}$ . Here, we used the same BSP envelope, but transformed to the  $(B - V)$  color using the Bessell (1979) relations. Parenthetically, we note that a more careful scrutiny of the photometric data than in CAL4 resulted in a better definition of the period – color relation. Except for the short-period system RW Com, all systems are located within the band marked in Figure 2.

The expected spread in the predicted values of  $M_V$  for CAL5, estimated from the Monte Carlo experiment described above, is shown in Figure 6. The continuous and broken lines give the spread in absolute magnitudes encompassing 68.3% and 95.4% of all cases; these intervals can be identified with one- and two-sigma ranges. As described above, the spread stems from the combined uncertainties in the coefficients and from the observed spread in  $(B - V)$ . It is surprisingly small indicating that, in principle, the standard mean error of predictions of  $M_V$  should be at the level of 0.1. The observed mean error is larger,  $\sigma = 0.22$  (vertical bar in Figure 6), indicating that the Monte Carlo estimated errors may give overly optimistic estimates. Of particular importance are three deviating systems with good parallaxes, V759 Cen, SW Lac and TY Men, which are clearly too bright than predicted by the calibration and which mainly contribute to the increase of the mean error  $\sigma$ . We have checked the input data for these three systems and see no obvious reason why they deviate and what is causing the high luminosities, since they also do not give any clear hints of a third, hidden parameter dependence, as will be discussed in Section 4.

#### 4. Do we see a third parameter in the luminosity calibration?

The new luminosity – period – color relation may be accurate enough to reveal systematic deviations of calibrating systems with properties deviating from the general trend. It was stated in CAL1 that the mass-ratio  $q$  would be the most likely third parameter in the calibration. Thus, we may expect that the calibration should be fully valid for systems with an “average value” of  $q$ , and that systems with mass-ratios deviating noticeably from the average value would show systematic residuals  $\Delta M_V$  from the calibrating plane. In addition to  $q$ , the fill-out factor  $f$  and the orbital inclination  $i$  may influence the luminosity to a certain extent. The first two,  $q$  and  $f$ , are related to structural properties and are known (Maceroni and van’t Veer 1996) to correlate with the spectral type and total mass (early type systems have usually small mass ratios and large fill-out factors), so that we might expect that their contributions are already absorbed in the color term.

We have collected the system parameters  $(q, f, i)$  for the majority of the systems used in CAL5. The data are given in Table 1, details on the source of data are given in the Appendix. The residuals  $\Delta M_V$  from the calibration are plotted versus each of these parameters in Figure 7. The formal linear fits, giving coefficients as in Table 3, indicate no significant dependencies for  $q$  and  $f$ ; this table gives also results of bootstrap re-sampling experiments. The lack of systematic trends is also obvious in Figure 7. Only the  $i$  dependence shows a 0.15 mag variation in the interval  $60^\circ$



to  $90^\circ$  which is well covered by observed systems, indicating the possibility of a gravity-induced brightening at the poles. The slope per degree,  $+0.0053_{-0.0041}^{+0.0027}$ , is significant at the level slightly higher than one-sigma. Since this effect is of the order of the accuracy of the calibration, it can be neglected in statistical studies.

In addition to the geometrical parameters ( $q, f, i$ ) one could consider metallicity as a hidden unknown of the calibration. Unfortunately, nothing is known about differences in metallicities within the sample of the local W UMa-type systems. Similarly, usage of any correlated indicators, such as spatial velocities, would not be advisable as one would expect a statistical rather than a deterministic relation between deviations in  $M_V$  and the values of the space velocity vectors.

## 5. The poor thermal contact and semi-detached systems

As was described in CAL1 and CAL4, the existence of a period – color relation causes an insufficient separation of the color and period dependencies so that the results crucially depend on the data for “outlying” systems which are contact systems with unusually long periods for their colors. Such systems appear close to the red-color (broken line) boundary in Figure 2. They are important as they can stabilize the solutions by lifting the period – color degeneracy. For the previous calibrations in CAL1 to CAL4, the system V371 Cep (NGC 188 V5) was used in this special role. The current Hipparcos sample defined by  $\epsilon M_V < 0.5$  includes a wide range of combinations of periods and colors, so that it is no longer necessary to rely on extreme systems such as V371 Cep. In fact, we are for the first time in a position to check if the calibration is indeed valid for such systems. As indicated by the OGLE data (Rucinski 1997b), the poor-thermal-contact (PTC) and possibly semi-detached (sd) systems mimicking good contact are very rare in space, constituting only some 2% of all contact systems. They are very important for our understanding of pre- and in-contact evolution. We used V371 Cep in the previous versions of the luminosity calibration to improve stability of solutions, but *it has never been proven that the luminosity calibrations of the CAL series are applicable to such systems at all!*

There are very few binaries with reliable values of  $M_V$  among the PTC/sd systems. In addition to V371 Cep, one can consider here RT Scl which seems to be a genuine semi-detached system (Hilditch and King 1986, Banks et al. 1990), perhaps also the red system RW Com (Milone et al. 1987) which is included in our calibration, although with very low weight. If we apply the new calibration to such systems, their absolute visual magnitudes (derived from spectroscopic and photometric analysis) are usually fainter than predicted. The deviations amount to 0.80 magnitude for V371 Cep, 0.40 magnitude for RT Scl, while RW Com deviates by as much as 0.95 magnitude.

The sample of the PTC/sd systems is clearly too small to draw definite conclusions, but we point out that low luminosities (for a given color) are actually expected for such systems. By comparing mixing of colors of Main Sequence stars (clearly the extreme case of no thermal contact) with colors of genuine contact systems, one sees that the PTC/sd systems should be always bluer than systems in good geometrical and thermal contact (Figure 8). The observed colors will obviously depend on how good or poor the thermal contact actually is, so that their

values cannot be predicted easily. But the result is clear: The luminosities estimated from the calibration are expected to be always too high, which seems to be confirmed by results described above. It would be of great importance to confirm this prediction on the basis of a larger sample of PTC/sd systems.

## 6. Conclusions

We have presented a luminosity calibration of contact binaries based on Hipparcos parallaxes, which covers a wide range in periods and colors. It is based on the  $(B - V)$  color index and supersedes previous calibrations based on that color index. It nominally predicts absolute magnitudes to an accuracy of  $\pm 0.1$ , although deviations of some systems are larger, indicating a wide, non-Gaussian distribution of uncertainties. For the current data, the weighted mean error is  $\sigma = 0.22$ . The calibration can be written as:

$$M_V = -4.44 \log P + 3.02(B - V)_0 + 0.12 \quad (5-a)$$

We have investigated the influence of mass-ratio, fill-out factor and inclination, and have found that the first two parameters are, within the accuracy of the calibration, completely absorbed by the color term. Only the inclination, which is independent of the physical configuration of a system, shows a noticeable effect, as it is expected from the gravity brightening. Nevertheless, this effect is so small that it can be neglected in statistical studies. Close binary systems appearing in the period domain of the W UMa-type systems, but showing unequally deep eclipses (either poor-thermal contact or semi-detached systems) appear too faint relative to the calibration by roughly 0.5 magnitude, but the sample is much too small to draw definite conclusions.

The accuracy of the present calibration is no longer limited by the parallax data but, paradoxically, by the lack of reliable photometric data. It should be noted that an uncertainty in the color index  $(B - V)$  of 0.03 contributes a deviation of 0.1 magnitude in the predicted  $M_V$ .

HWD gratefully acknowledges support from the sabbatical visitors program at Space Telescope Science Institute and SMR acknowledges a research grant from the Natural Sciences and Engineering Council of Canada. The research has made use of the SIMBAD database, operated at the CDS, Strasbourg, France.

## Appendix: Sources of input data

In the following, information is given on the source of apparent magnitudes at maximum, color indices and system parameters of the W UMa systems used in CAL5.

**AB And.**  $V$  magnitude and  $(B - V)$  index from Landolt (1969). He quotes  $(B - V) = 0.90$  as the color index at total eclipse. Using the color index of the comparison, and differential colors of the contact system, we get 0.865 for the (fairly poorly determined) maximum and 0.90 for the minimum. The  $(b - y)$ -index suggests  $(B - V) = 0.88$ , which was adopted for CAL5. The system parameters were taken from the detailed study of Hrivnak (1988),

**S Ant.**  $V$  and  $(B - V)$  from Popper (1957), system parameters from Russo et al. (1982).

**V535 Ara.**  $V$  and  $(B - V)$  from Schöffel (1979), system parameters are averages of the values given by Schöffel (1979) and Leung and Schneider (1978).

**TZ Boo.** This system shows a very unstable light curve.  $V$  and  $(B - V)$  averaged from data by Hoffmann (1978), mass ratio given by McLean and Hilditch (1983), inclination estimated by Al-Naimiy and Jabbar (1987).

**AC Boo.**  $(B - V)$  given by Mauder (1964). Several  $B$ ,  $V$  light curves are available, but none refers to a comparison star with known  $B$ ,  $V$  magnitudes. The  $V$  magnitude at maximum was calculated from the  $H_p$  magnitude. Mass ratio from Hrivnak (1993), inclination and fill-out factor from Mancuso et al. (1978).

**CK Boo.** Aslan and Derman (1986) measured  $UBV$  light curves relative to HD 128128. Strömgren photometry of HD 128128 (Olsen 1994) yields  $V = 7.897$ ,  $b - y = 0.348$ , from which  $(B - V) = 0.55$  was derived. Mass ratio from Hrivnak (1993).

**RR Cen.**  $V$  and  $(B - V)$  from Chambliss (1971), system parameters averaged from Mochnacki and Doughty (1972) and King and Hilditch (1984).

**V752 Cen.**  $V$  and  $(B - V)$  from Sistero and Castore de Sistero (1973), also  $(B - V)$  from Duerbeck (1997). Averaged color index used here. System parameters taken from Barone et al. (1993).

**V757 Cen.**  $V$  and  $(B - V)$  from Cerruti and Sistero (1982), also  $(B - V)$  from Duerbeck (1997). Averaged color index used here. System parameters taken from Maceroni, Milano and Russo (1984).

**V759 Cen.**  $(B - V)$  was derived from Bond's (1970)  $b - y$  value. Maximum  $V$  magnitude was calculated from the  $H_p$  magnitude.

**VW Cep.** Linnell (1982) gives  $B$ ,  $V$  light curves relative to BD +74° 889, whose  $B$ ,  $V$  magnitudes were taken from Sorgsepp and Albo (1974). System parameters were taken from Hill (1989) and Mochnacki (1981).

**RS Col.**  $V$  and  $(B - V)$  from McFarlane and Hilditch (1987), who also determined system parameters.

**RW Com.**  $V$  and  $(B - V)$  from Milone et al. (1980), system parameters from Milone, Wilson and Hrivnak (1987).

$\epsilon$  **CrA.**  $V$  and  $(B - V)$  from Tapia (1969), mass ratio from Goecking and Duerbeck (1993), inclination and fill-out factor by Tapia and Whelan (1975).

**SX Crv.**  $V$  and  $(B - V)$  are averaged from Sanwal et al. (1974) and Scaltriti and Busso (1984).

**V1073 Cyg.** The  $(B - V)$  index is given by Mendoza, Gómez, & González (1978). Several light curves are available, but none refers to a comparison star with known  $B$ ,  $V$  magnitudes. The  $V$  magnitude at maximum was calculated from the  $H_p$  magnitude. The system parameters were taken from the study of Ahn, Hill and Khalessheh (1992).

**RW Dor.**  $V$  and  $(B - V)$  from Marton, Grieco and Sistero (1989), who also give system parameters. The parameters used here are average values of the previous study and that of Kaluzny and Caillault (1989).

**AP Dor.**  $V$  magnitude at maximum estimated from Eggen’s (1980) observations,  $(B - V)$  taken from Przybylski and Kennedy (1965).

**BV Dra** and **BW Dra.**  $V$  and  $(B - V)$  averaged from Yamasaki (1979) and Rucinski and Kaluzny (1982). The system parameters were taken from Kaluzny and Rucinski (1986).

**YY Eri.**  $V$  at maximum calculated from the  $H_p$  magnitude.  $(B - V)$  taken from Eggen (1967). System parameters were derived by Nesci et al. (1986).

**SW Lac.**  $V$  and  $(B - V)$  from Rucinski (1968). System parameters were derived by Leung, Zhai and Zhang (1984).

**XY Leo.**  $V$  from Hrivnak (1985). The  $(B - V)$  index is an average of the determinations of Koch (1974), Hrivnak (1985), and Duerbeck (1997). System parameters were derived by Hrivnak (1985) and Barden (1987). The latter found that XY Leo is a quadruple system. The  $V$  magnitude has been increased by 0.05 to account for the M-type pair.

**AP Leo.**  $V$  at maximum calculated from the  $H_p$  magnitude.  $(B - V)$  taken from Duerbeck (1997). System parameters were derived by Zhang, Zhang and Zhai (1992).

**UV Lyn.**  $V$  and  $(B - V)$  from Bossen (1973). A more recent derivation of system parameters was carried out by Markworth and Michaels (1982).

**TY Men.** Naqvi and Grønbech (1976) obtained *uvby* light curves.  $V$  magnitude averaged from both maxima;  $(B - V)$  calculated from average  $(b - y)$  index. The system parameters were derived by Lapasset (1980).

**UZ Oct.**  $V$  and  $(B - V)$  taken from Castore de Sistero, Sistero and Candellero (1979). The system parameters were derived by Lapasset and Sistero (1984).

**V502 Oph.**  $V$  and  $(B - V)$  taken from Wilson (1967). System parameters are averaged from results of King and Hilditch (1984) and Maceroni et al. (1982).

**V566 Oph.** Lafta and Grainger (1985) give  $B, V$  photometry relative to BD +4° 3558, whose *UBVRI* photometry is given by Castelaz et al. (1991). System parameters are averaged from results of Van Hamme and Wilson (1985) and Mochnacki and Doughty (1972).

**V839 Oph.** Several  $B, V$  light curves are available, but none refers to a comparison star with known  $B, V$  magnitudes.  $V$  at maximum was derived from the  $H_p$  magnitude.  $(B - V)$  is an average of the value published by Koch (1974) and that calculated from the  $(b - y)$  index determined by Rucinski and Kaluzny (1981). The inclination is taken from an analysis by Niarchos (1989).

**MW Pav.**  $V$  and  $(B - V)$  from Lapasset (1977), system parameters taken from Lapasset (1980).

**U Peg.** No light curve relative to a comparison star with known  $B, V$  magnitudes exists.  $V$  at maximum was derived from the  $H_p$  magnitude.  $(B - V)$  was taken from Eggen (1967), system

parameters from the study of Zhai and Lu (1988).

**AE Phe.**  $V$  and  $(B - V)$  from Walter and Duerbeck (1988), system parameters were averaged from the results of Van Hamme and Wilson (1985) and Niarchos and Duerbeck (1991).

**VZ Psc.**  $V$  at maximum was extrapolated from Bradstreet’s (1985) fragmentary  $UBVRI$  observations. Several measurements of  $(B - V)$  are available; a “median” value is that measured by Ryan (1989). System parameters were determined by Hrivnak, Guinan and Lu (1995).

**AQ Psc.**  $V$  and  $(B - V)$  from Sarma and Radhakrishnan (1982).

**HI Pup.**  $V$  at maximum was calculated from the  $H_p$  magnitude,  $(B - V)$  was taken from Duerbeck (1997).

**V781 Tau.**  $V$  and  $(B - V)$  from Cereda et al. (1988). System parameters were determined by Lu (1993).

**W UMa.** We used the  $B$ ,  $V$  light curves by Breinhorst (1971), which were measured relative to BD +56° 1399, for which Oja (1984) gives  $UBV$  magnitudes. System parameters were taken from the study of Linnell (1991).

**AW UMa.**  $V$  and  $(B - V)$  from Paczynski (1964). System parameters were averaged from the studies by Rucinski (1992) and Hrivnak (1982).

**GR Vir.**  $V$  and  $(B - V)$  from Cereda et al. (1988).

## REFERENCES

- Ahn, Y.S., Hill, G., and Khalessheh, B. 1992, *A&A*, 265, 597
- Al-Naimiy, H.M.K., and Jabbar, S.R. 1987, *Ap&SS*, 134, 153
- Aslan, Z., and Derman, E. 1986, *A&AS*, 66, 281
- Baade, D., Duerbeck, H.W., Karimie, M.T., and Yamasaki, A. 1983, *Ap&SS*, 93, 69
- Banks, T., Sullivan, D.J. and Budding, E. 1990, *Ap&SS*, 173, 77
- Barden, S.J. 1987, *ApJ*, 317, 333
- Barone, F., Di Fiore, L., Milano, L., and Russo, G. 1993, *ApJ*, 407, 237
- Bessell, M.S. 1979, *PASP*, 91, 589
- Bohlin, R.C., Savage, B.D., and Drake, J.F. 1978, *ApJ*, 224, 132
- Bond, H.E. 1970, *PASP*, 82, 1065
- Bossen, H. 1973, *A&A*, 10, 217
- Bradstreet, D.H. 1985, *ApJS*, 58, 413
- Breinhorst, R.A. 1971, *Ap&SS*, 10, 411
- Castelaz, M.W., Persinger, T., Stein, J.W., Prosser, J., and Powell, H.D. 1991, *AJ*, 102, 2103
- Cereda, L., Mistò, A., Niarchos, P.G., and Poretti, E. 1988, *A&AS*, 76, 255

- Cerruti, M.A., and Sistero, R.F. 1982, *PASP*, 94, 189
- Chambliss, C.R. 1971, *AJ*, 76, 64
- Duerbeck, H.W. 1984, *Ap&SS*, 99, 363
- Duerbeck, H.W. 1997, unpublished material
- Eggen, O.J. 1967, *MemRAS*, 70, 111
- Eggen, O.J. 1980, *IBVS*, 1772
- Edmonds, P. D., Gilliland, R. L., Guhathakurta, P., Petro, L. D., Saha, A., and Shara, M. M. 1996, *ApJ*, 468, 241
- ESA, 1997, *The Hipparcos and Tycho Catalogues*, ESA SP-1200
- Fruscione, A., Hawkins, I., Jelinsky, P., and Wiercigroch, A. 1994, *ApJS*, 94, 127
- Goecking, K.-D., and Duerbeck, H.W. 1993, *A&A*, 278, 463
- Goecking, K.-D., Duerbeck, H.W., Plewa, T., Kaluzny, J., Schertl, D., Weigelt, G., and Flin, P. 1994, *A&A*, 289, 827
- Hilditch, R.W., Hill, G., and Bell, S.A. 1992, *MNRAS*, 255, 285
- Hilditch, R.W. and King, D.J. 1986, *MNRAS*, 223, 581
- Hill, G. 1989, *A&A*, 218, 141
- Hoffmann, M. 1978, *A&AS*, 33, 63
- Hrivnak, B.J. 1982, *ApJ*, 260, 744
- Hrivnak, B.J. 1985, *ApJ*, 290, 696
- Hrivnak, B.J. 1988, *ApJ*, 335, 319
- Hrivnak, B.J. 1993, in *New Frontiers in Binary Star Research*, ASP Ser. No. 38, eds. K.-C. Leung and I.-S. Nha, p. 274
- Hrivnak, B.J., Guinan, E.F., and Lu, W. 1995, *ApJ*, 455, 300
- Kaluzny, J., and Caillault, J.-P. 1989, *AcA* 39, 27
- Kaluzny, J., Krzemiński, W., and Mazur, B. 1996a, *A&A*, 118, 303
- Kaluzny, J., Kubiak, M., Szymanski, M., Udalski, A., Krzemiński, W., and Mateo, M. 1996b, *A&AS*, 120, 139
- Kaluzny, J., and Rucinski, S.M. 1986, *AJ*, 92, 666
- King, D.J., and Hilditch, R.W. 1984, *MNRAS*, 209, 645
- Koch, R.H. 1974, *AJ*, 79, 34
- Lafta, S.J., and Grainger, J.F. 1985, *Ap&SS*, 114, 23
- Landolt, A.U. 1969, *AJ*, 74, 1078
- Lapasset, E. 1977, *Ap&SS*, 46, 155
- Lapasset, E. 1980, *AJ*, 85, 1098
- Lapasset, E., and Sistero, R.F. 1984, *A&A*130, 97

- Leung, K.-C., and Schneider, D.P. 1978, *ApJ*, 211, 853
- Leung, K.-C., Zhai, D.-S., and Zhang, R.-X. 1984, *PASP*, 96, 634
- Linnell, A.P. 1982, *ApJS*, 50, 85
- Linnell, A.P. 1991, *ApJ*, 374, 307
- Lu, W. 1993, *AJ*, 105, 646
- Maceroni, C., Milano, L., and Russo, G. 1982, *A&AS*, 49, 123
- Maceroni, C., Milano, L., and Russo, G. 1984, *A&AS*, 58, 405
- Maceroni, C., and Van't Veer, F. 1996, *A&A*, 311, 523
- McFarlane, T.M., and Hilditch R.W. 1987, *MNRAS*, 227, 389
- McLean, B.J., and Hilditch, R.W. 1983, *MNRAS*, 203, 1
- Mancuso, S., Milano, L., and Russo, G. 1978, *A&A*, 63, 193
- Markworth, N.L., and Michaels, E.J. 1982, *PASP*, 94, 350
- Marton, S.F., Grieco, A., and Sistero, R.F. 1989, *MNRAS*, 240, 931
- Mauder, H. 1964, *ZAp*, 60, 222
- Mazur, B., Krzemiński, W., and Kaluzny, J. 1995, *MNRAS*, 273, 59
- Mendoza V., E.E., Gómez, T., and González, S. 1978, *AJ*, 83, 606
- Milone, E.F., Chia, T.T., Castle, K.G., Robb, R.M., and Merrill, J.E. 1980, *ApJS*, 43, 339
- Milone, E.F., Wilson, R.E., and Hrivnak, B.J. 1987, *ApJ*, 319, 325
- Mochnicki, S.W. 1981, *ApJ*, 245, 650
- Mochnicki, S.W., and Doughty, N.A. 1972, *MNRAS*, 156, 243
- Nagy, T.A. 1977, *PASP*, 89, 366
- Naqvi, S.I.H., and Grønbech, B., 1976, *A&A*, 47, 315
- Nesci, R., Maceroni, C., Milano, L., and Russo, G. 1986, *A&A*159, 142
- Niarchos, P.G. 1989, *Ap&SS*, 153, 143
- Niarchos, P.G., and Duerbeck, H.W. 1991, *A&A*, 247, 399
- Oja, T. 1984, *A&AS*, 57, 357
- Olsen, E.H. 1994, *A&AS*, 106, 257
- Paczynski, B. 1964, *AJ*, 69, 124
- Popper, D.M. 1957, *ApJ*, 124, 208
- Predehl, P., and Schmitt, J.H.M.M. 1995, *A&A*, 293, 889
- Przybylski, A., and Kennedy, P.M. 1965, *MNRAS*, 129, 63
- Rubinstein, E.P., and Bailyn, C.D. 1996, *AJ*, 111, 260
- Rucinski, S.M. 1968, *AcA*, 18, 49
- Rucinski, S.M. 1983, *A&A*, 127, 84

- Rucinski, S.M. 1985, in *Interacting Binary Stars*, eds. J.E. Pringle, R.A. Wade, Cambridge: Cambridge Univ. Press, pp. 85 and 113
- Rucinski, S.M. 1992, *AJ*, 104, 1968
- Rucinski, S.M. 1993, in *The Realm of Interacting Binary Stars*, eds. J. Sahade, Y. Kondo, G. McClusky, Dordrecht: Kluwer Academic Publishers, p. 111
- Rucinski, S.M. 1994, *PASP*, 106, 462 (CAL1)
- Rucinski, S.M. 1995, *PASP*, 107, 648 (CAL2)
- Rucinski, S.M. 1996, in *The Origins, Evolution, and Destinies of Binary Stars in Clusters*, eds. E.F. Milone and J.-C. Mermilliod, *ASP Conf. 90*, 270
- Rucinski, S.M. 1997a, *AJ*, 113, 407 (CAL3)
- Rucinski, S.M. 1997b, *AJ*, 113, 1112
- Rucinski, S.M., and Duerbeck, H.W. 1997, *Proc. Hipparcos Venice Conf.*, ESA SP (in press) (CAL4)
- Rucinski, S.M., and Kaluzny, J. 1981, *AcA*, 31, 409
- Rucinski, S.M., and Kaluzny, J. 1982, *Ap&SS*, 88, 433
- Russo, G., Sollazzo, C., Maceroni, C., and Milano, L. 1982, *A&AS*, 47, 211
- Ryan, S.G. 1989, *AJ*, 98, 1693
- Sanwal, N.B., Sarma, M.B.K., Parthasarathy., M., and Abhyankar, K.D. 1974, *A&AS*, 13, 81
- Sarma, M.B.K., and Radhakrishnan, K.R. 1982, *IBVS* 2073
- Scaltriti, F., and Busso, M. 1984, *A&A*, 135, 23
- Schöffel, E. 1979, *A&AS*, 36, 287
- Sistero, R.F., and Castore de Sistero, M.E. 1973, *AJ*, 78, 413
- Sistero, R.F., Castore de Sistero, M.E., and Candellero, B. 1979, *A&AS*, 38, 171
- Sorgsepp, L., and Albo, C. 1974, *Publ. Tartu Ap. Obs.*, 42, 103
- Tapia, S. 1969, *AJ*, 74, 533
- Tapia, S., and Whelan, J. 1975, *ApJ*, 200, 98
- Tinbergen, J. 1982, *A&A*, 105, 53
- Turon, C., Norin, D., Arenou, F., and Perryman, M. A. C 1994, *Hipparcos Input Catalogue*, CD-ROM Version (INCA Consortium)
- Van Hamme, W., and Wilson, R.E. 1985, *A&A*152, 25
- Walter, K. and Duerbeck, H.W. 1988, *A&A*, 189, 89
- Whittet, D.C.B. 1992, *Dust in the Galactic Environment* (Inst. of Physics Publ., Bristol)
- Wilson, R.E. 1967, *AJ*, 72, 1028
- Yamasaki, A. 1979, *Ap&SS*, 60, 173
- Yan, L., and Mateo, M. 1994, *AJ*, 108, 1810



Zhai, D.-S., and Lu, W.-X. 1988, *Ac. As. Sin.* 29, 9 = *Ch. A& Ap* 12, 223

Zhang, J.-T., Zhang, R.-X., and Zhai. D.-S. 1992, *Ac. As. Sin.* 33, 131 = *Ch. A& Ap* 16, 407

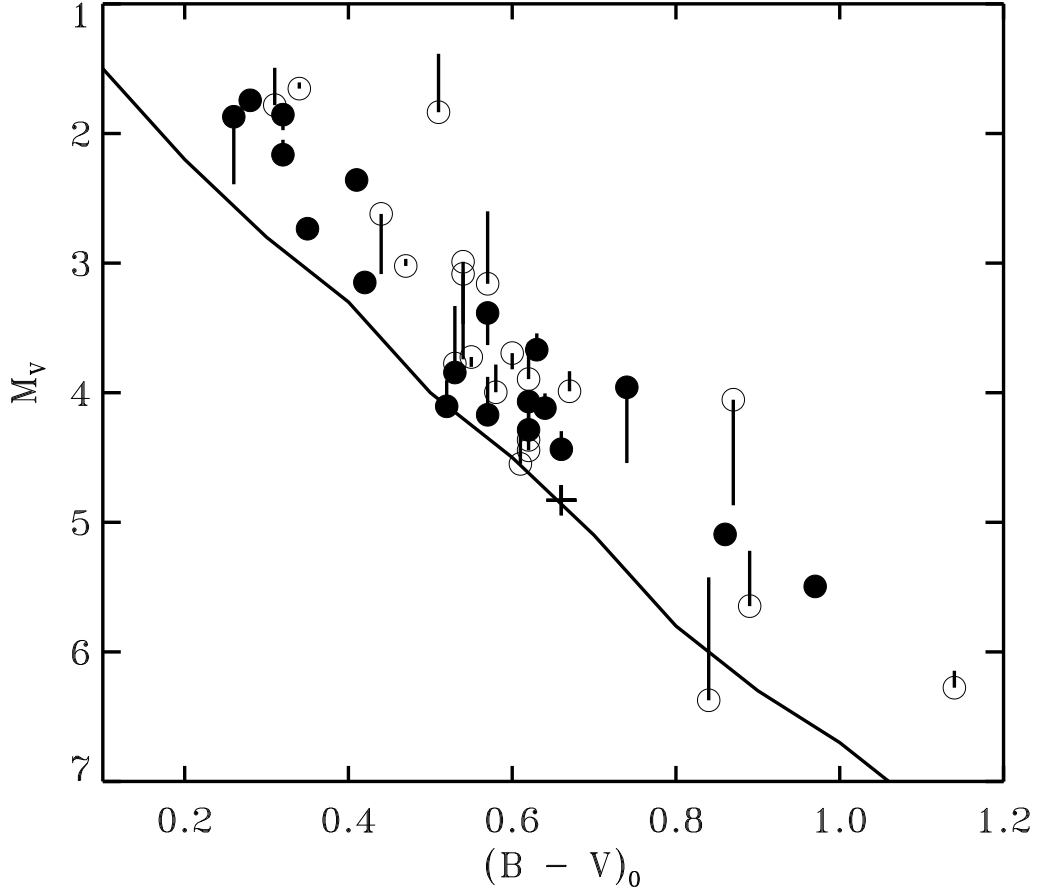


Fig. 1.— The color – magnitude relation for the Hipparcos systems with absolute-magnitude errors smaller than 0.25 magnitude (filled circles) and within 0.25 to 0.5 magnitude (open circles). The same symbols are used in all subsequent figures. The line gives the main sequence for single solar-type stars, with the Sun marked by a cross. The short vertical vectors point at locations predicted by the new calibration presented in this paper called CAL5.

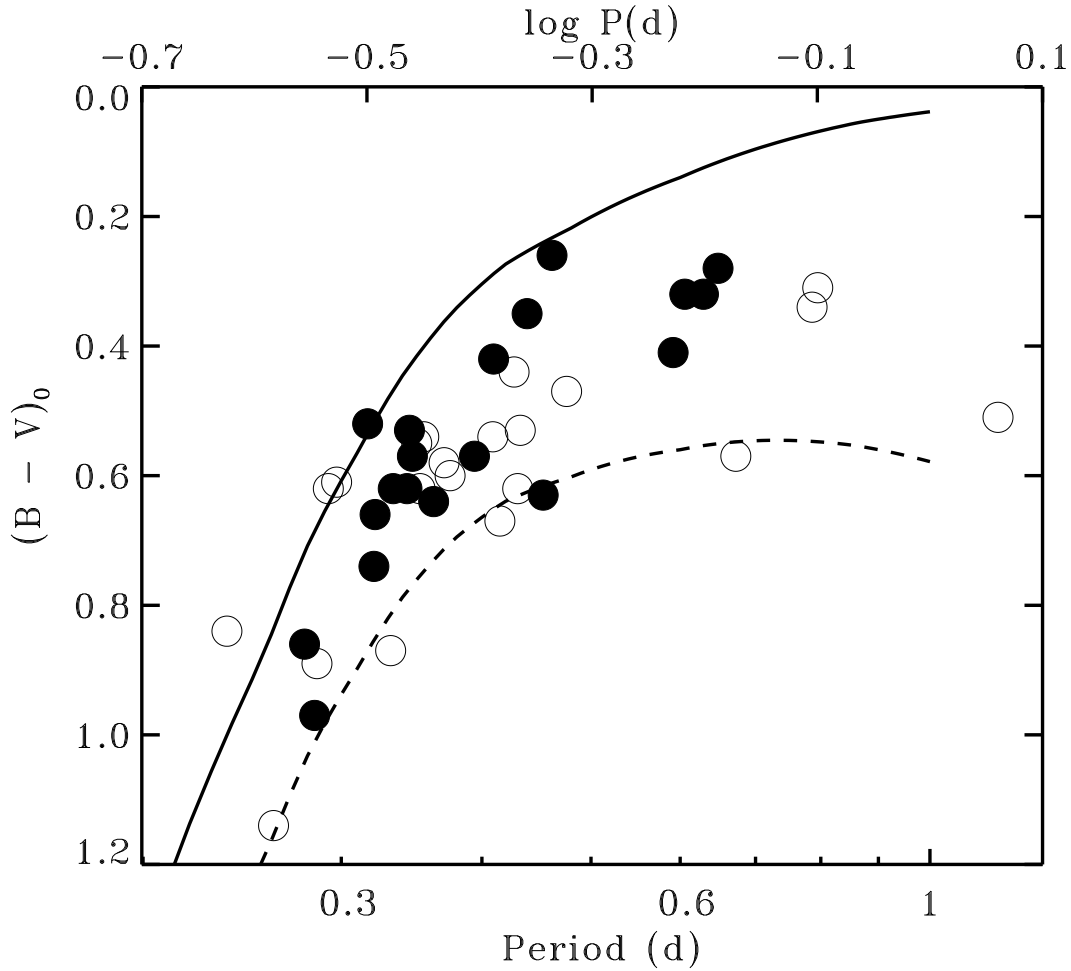


Fig. 2.— The period – color diagram for the W UMa-type systems observed by Hipparcos (filled and open circles, as in Figure 1). The solid line is the blue–short–period envelope (BSPE) from CAL3, transformed to the  $(B - V)$  color. The broken line gives the red edge of the band which was used in a Monte Carlo experiment to estimate the spread in  $M_V$ . Its location was roughly estimated to include evolved systems with red colors (for a given period). The red edge was constructed by adding a linearly-increasing value to the BSPE, so that the band would widen from 0.3 at 0.2 days to 0.6 at 1.0 day. The BSPE is poorly defined for periods longer than about 0.6 – 0.7 day.

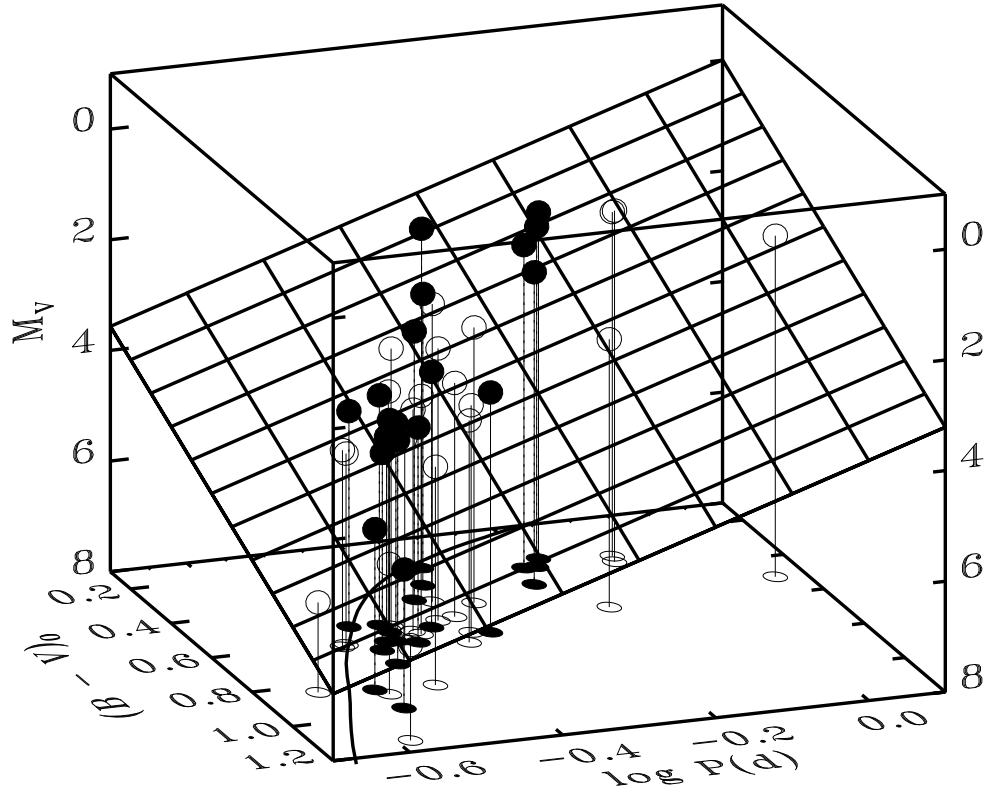


Fig. 3.— The period – color – luminosity relation for the Hipparcos systems. The inclined surface gives the new calibration CAL5. The mean weighted deviation of the observed points from the calibration plane is  $\sigma = 0.22$ . The data projected onto the horizontal period – color plane yield the same period – color relation as in Figure 2.

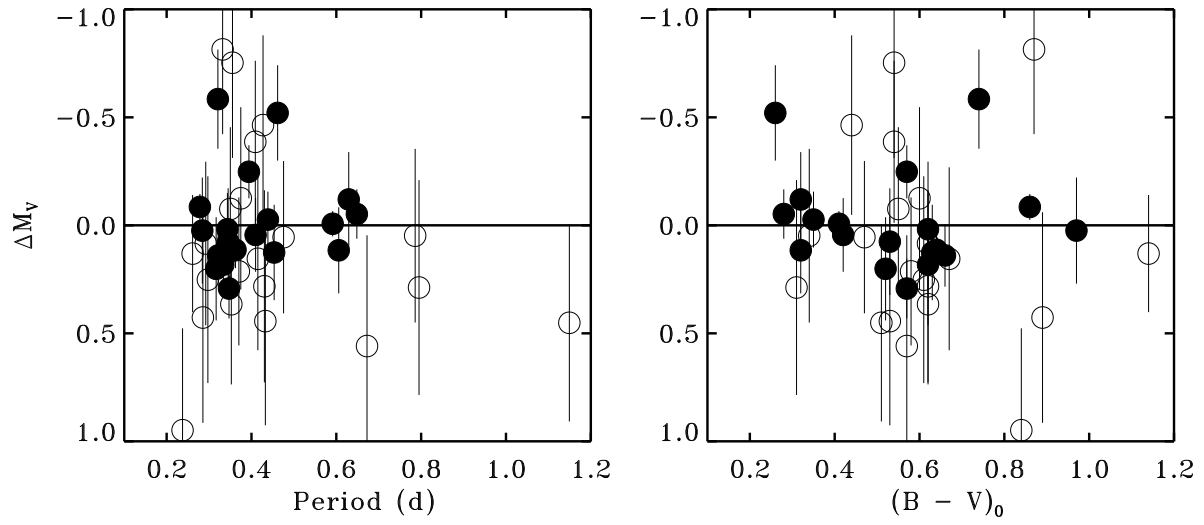


Fig. 4.— Deviations from the new calibration CAL5 are shown here as functions of the two principal parameters. The vertical error bars have lengths equal to twice the absolute-magnitude errors, as estimated from the uncertainties in the Hipparcos parallaxes.

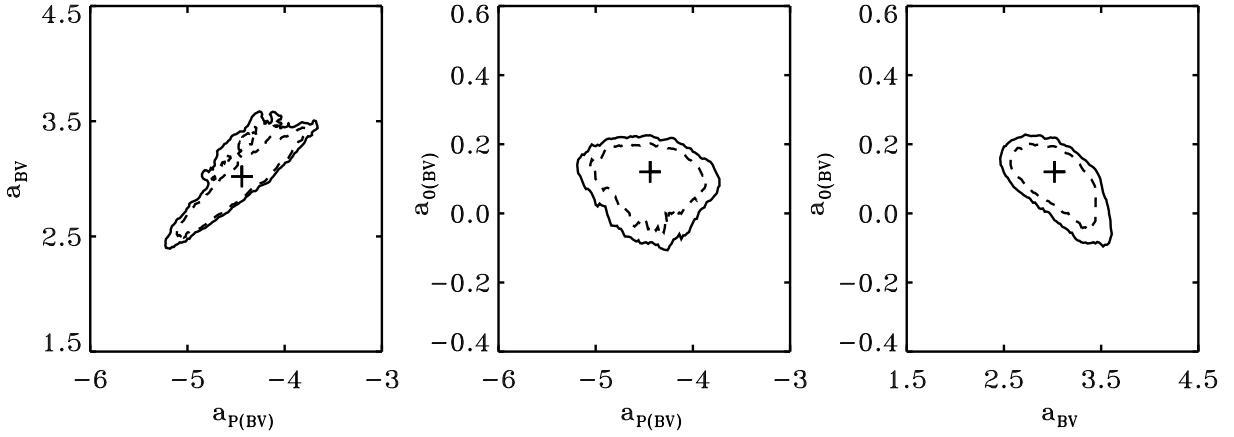


Fig. 5.— Relations between the coefficients of the new calibration CAL5 established by a bootstrap re-sampling experiment. The naming of the coefficients is the same as in CAL1, in that BV in parentheses indicates that this is a  $(B - V)$ -based calibration. The solid contours encompass 68.3% of all bootstrap solutions of the coefficients, a level which is normally associated with the one-sigma standard-error uncertainty. The dotted lines give similar levels for 50%, which is normally associated with the probable errors. Note that separate “islands” in mutual correlations between the coefficients – which were present in the previous calibrations – no longer exist indicating higher stability of the present solutions.

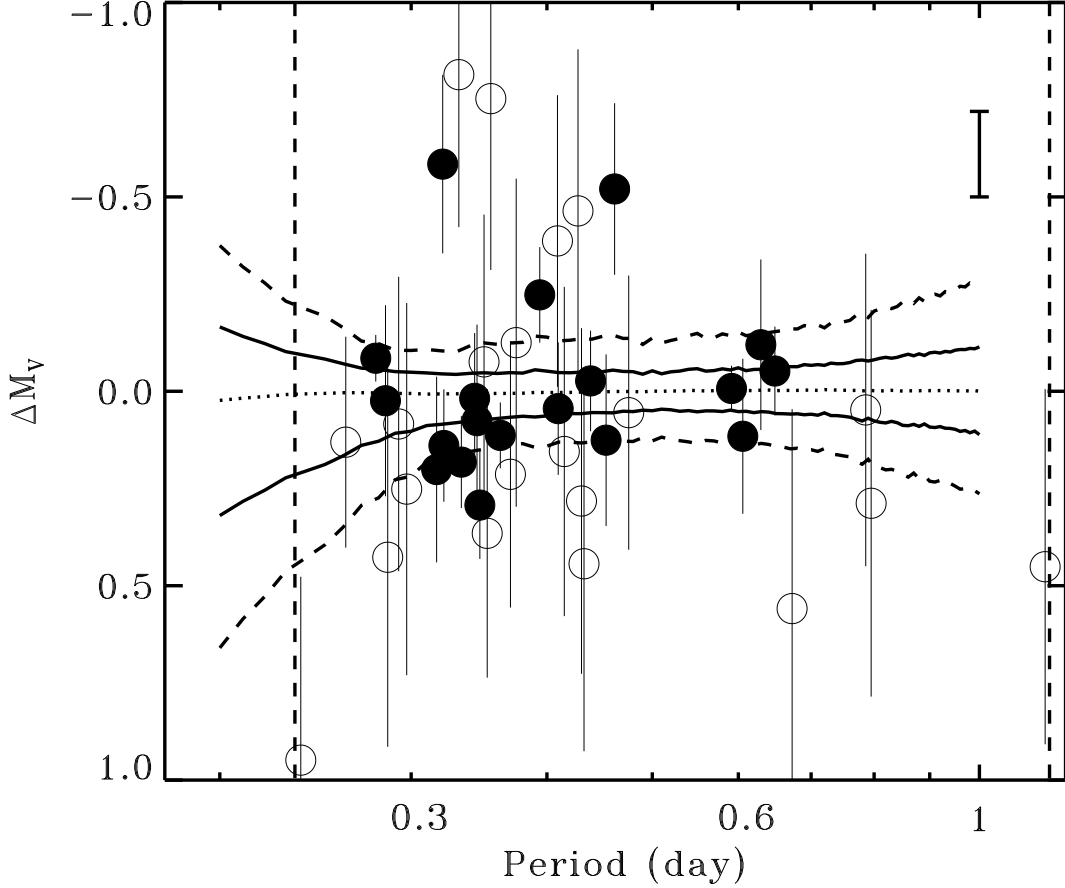


Fig. 6.— The spread in the predicted values of  $M_V$  obtained from a Monte Carlo experiment for CAL5 is shown here by curves. It was derived by combining the spread in the calibration coefficients, as shown in Figure 5, with an assumed spread in colors. In practice, 10,000 calibration coefficients obtained in the bootstrap experiments were applied to 100 uniformly distributed random values of the colors (within ranges shown in Figure 2) for each value of the period in steps of 0.01 day. The solid lines give the one-sigma range (68.3% of all cases), whereas the broken lines give the two-sigma range (95.4% of all cases). The median for the random samplings is shown by the dotted line. The two vertical broken lines delineate the region defined by systems with the extreme values of the orbital period in the Hipparcos sample. The vertical bar gives the weighted mean deviation in the sample,  $\sigma = 0.22$ . The filled and open circles as well as the vertical bars have the same meanings as in other figures.

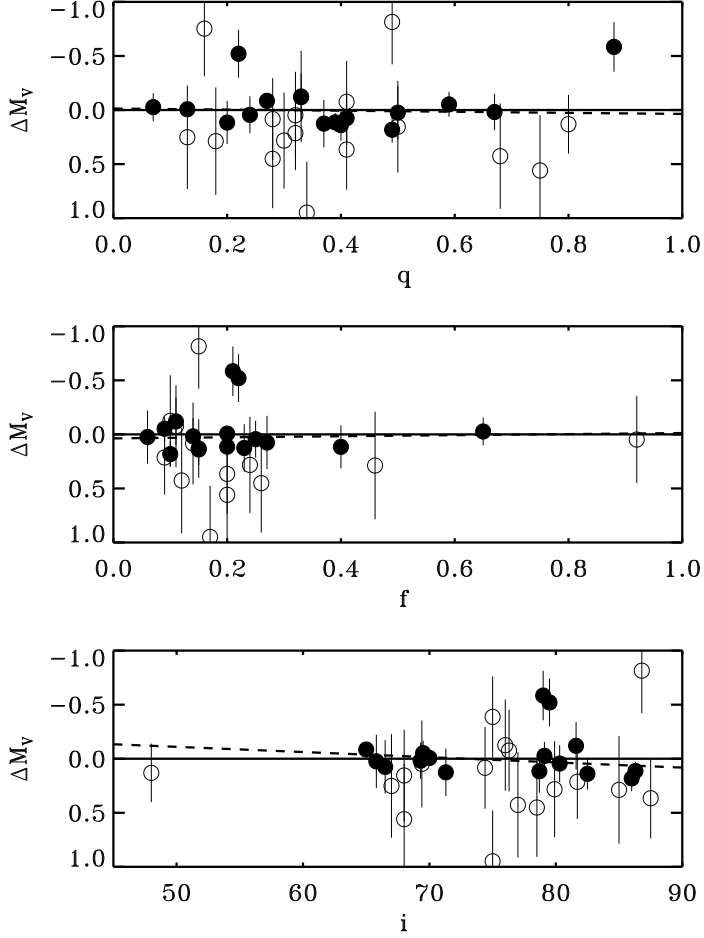


Fig. 7.— Deviations from the calibration are shown here versus the physical parameters of the contact system: the mass ratio,  $q = M_2/M_1 \leq 1$ , the fill-out parameter,  $f$ , defined through equipotentials with  $f = 0$  for the inner common equipotential, and the orbital inclination,  $i$ , in degrees. The filled and open circles as well as the vertical bars have the same meanings as in previous figures. The dashed lines indicate the weighted least squares fits to the data. Note that  $(q, f, i)$  data are not available for all systems studied here.



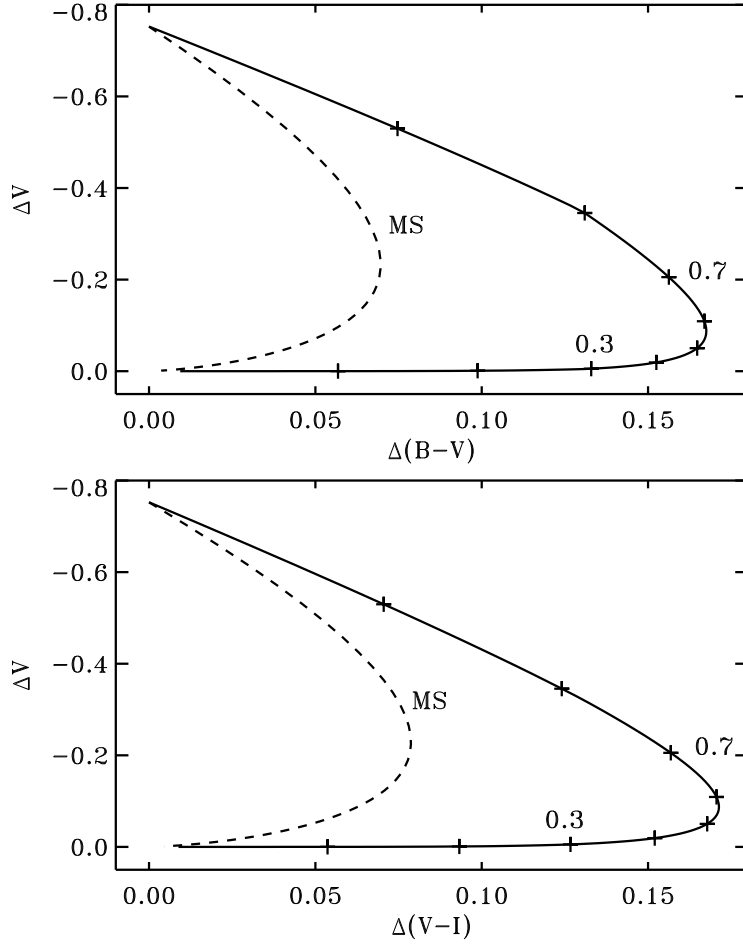


Fig. 8.— Expected changes in  $V$  and  $(B - V)$  (upper panel) and  $V$  and  $(V - I)$  (lower panel) for good-thermal contact systems with the varying mass-ratio,  $q$ , are shown by the continuous lines with marks every 0.1 in  $q$ . The broken lines show simple mixing of colors for Main Sequence stars which can be taken as an extreme case of poor thermal contact. The calculations presented here are for the color of the primary component  $(B - V) = 0.75$  and  $(V - I) = 0.8$  and assume the slope of the Main Sequence  $M_V \propto 4.85(B - V)$  and  $M_V \propto 4.35(V - I)$ . The color changes for good thermal-contact systems have been computed following the analysis of Mochnacki (1981) assuming the nuclear mass – luminosity relation  $L \propto M^{+4.4}$ . Note that the largest color changes are observed for  $0.5 < q < 0.6$ , and that they are accompanied by very small changes in brightness. Apparently, for such mass-ratios, the contact systems have secondaries contributing large radiating areas, but almost no luminosity. For  $q \rightarrow 0$  the systems resemble single stars, whereas for  $q \rightarrow 1$  the stars again influence each other to a lesser degree as they become identical, with the combined  $\Delta V \rightarrow -0.75$ . The poor thermal contact systems are expected to be located between the continuous and broken curves in the figure.

Table 1. Contact binary stars observed by Hipparcos with  $\epsilon M_V \leq 0.5$

Name	$P$	$B - V$	$E_{B-V}$	$V_{\max}$	$Hp_{\max}$	$q$	$f$	$i$	$\pi$	$\epsilon\pi$	$\epsilon M_V$	$M_V$	$\Delta M_V$
AB And	0.3319	0.88	0.01	9.49	9.68	0.49	0.15	86.6	8.3	1.5	0.39	4.05	-0.81
S Ant	0.6484	0.33	0.05	6.28	6.37	0.59	0.09	69.5	13.3	0.7	0.11	1.74	-0.05
V535 Ara	0.6293	0.34	0.02	7.17	7.24	0.33	0.11	81.6	8.9	0.9	0.22	1.85	-0.12
TZ Boo	0.2972	0.64	0.03	10.48	10.57	0.13	...	67.0	6.8	1.5	0.48	4.55	+0.25
AC Boo	0.3524	0.62	0.00	9.96	10.09	0.41	0.20	87.5	7.6	1.3	0.37	4.36	+0.37
CK Boo	0.3552	0.55	0.01	8.99	9.09	0.16	...	...	6.4	1.3	0.44	2.99	-0.75
RR Cen	0.6057	0.34	0.02	7.27	7.40	0.20	0.40	78.7	9.8	0.9	0.20	2.16	+0.12
V752 Cen	0.3702	0.60	0.02	9.17	9.20	0.32	0.09	81.7	9.5	1.5	0.34	4.00	+0.21
V757 Cen	0.3432	0.65	0.03	8.40	8.50	0.67	0.14	69.3	14.2	1.1	0.17	4.07	+0.02
V759 Cen	0.3939	0.59	0.02	7.44	7.56	...	...	...	15.9	0.9	0.12	3.38	-0.25
VW Cep	0.2783	0.86	0.00	7.30	7.54	0.27	0.00	65.0	36.2	1.0	0.06	5.09	-0.09
RS Col	0.6724	0.59	0.02	9.52	9.61	0.75	0.20	68.0	5.5	1.3	0.51	3.16	+0.56
RW Com	0.2375	0.84	0.00	11.07	11.24	0.34	0.17	75.0	11.5	2.5	0.47	6.37	+0.95
$\epsilon$ CrA	0.5914	0.41	0.00	4.74	4.82	0.13	0.20	70.0	33.4	0.9	0.06	2.36	-0.01
SX Crv	0.3166	0.54	0.02	8.98	9.05	...	...	...	10.9	1.2	0.24	4.11	+0.20
V1073 Cyg	0.7859	0.42	0.08	8.24	8.33	0.32	0.92	69.4	5.4	1.0	0.40	1.65	+0.05
RW Dor	0.2855	0.89	0.00	10.90	11.07	0.68	0.12	77.0	8.9	2.0	0.49	5.65	+0.43
AP Dor	0.4272	0.44	0.00	9.26	9.37	...	...	...	4.7	0.9	0.42	2.62	-0.46
BV Dra	0.3501	0.56	0.01	7.89	7.94	0.41	0.11	76.3	14.9	2.6	0.38	3.72	-0.08
BW Dra	0.2922	0.63	0.01	8.61	...	0.28	0.14	74.4	14.9	2.6	0.38	4.44	+0.08
YY Eri	0.3215	0.66	0.00	8.16	8.30	0.40	0.15	82.5	18.0	1.2	0.14	4.44	+0.14
SW Lac	0.3207	0.75	0.01	8.54	8.80	0.88	0.21	79.0	12.3	1.3	0.23	3.96	-0.58
XY Leo	0.2841	0.99	0.02	9.55	9.64	0.50	0.06	65.8	15.9	1.8	0.25	5.49	+0.02
AP Leo	0.4304	0.62	0.00	9.30	9.43	0.30	0.24	79.9	8.3	1.7	0.44	3.90	+0.28
UV Lyn	0.4150	0.67	0.00	9.42	9.58	0.50	...	68.0	8.2	1.6	0.42	3.99	+0.15
TY Men	0.4617	0.29	0.03	8.11	8.17	0.22	0.22	79.5	5.9	0.6	0.22	1.87	-0.52
UZ Oct	1.1494	0.54	0.03	9.03	9.14	0.28	0.26	78.5	3.8	0.8	0.46	1.84	+0.45
V502 Oph	0.4534	0.64	0.01	8.34	8.51	0.37	0.23	71.3	11.8	1.2	0.22	3.67	+0.13
V566 Oph	0.4096	0.43	0.01	7.45	7.55	0.24	0.25	80.3	14.0	1.1	0.17	3.15	+0.04
V839 Oph	0.4090	0.63	0.09	8.82	8.96	...	...	75.0	8.1	1.4	0.38	3.08	-0.39
MW Pav	0.7950	0.36	0.05	8.53	8.71	0.18	0.46	85.0	4.8	1.1	0.50	1.78	+0.29
U Peg	0.3748	0.62	0.02	9.47	9.60	0.33	0.10	76.0	7.2	1.4	0.42	3.69	-0.13
AE Phe	0.3624	0.64	0.00	7.56	7.69	0.39	0.20	86.3	20.5	0.8	0.08	4.12	+0.11
VZ Psc	0.2612	1.14	0.00	10.15	10.33	0.80	0.15	48.0	16.8	2.1	0.27	6.28	+0.13
AQ Psc	0.4756	0.50	0.03	8.60	8.66	...	...	...	8.0	1.3	0.35	3.02	+0.05
HI Pup	0.4326	0.60	0.07	10.33	10.46	...	...	...	5.4	1.2	0.48	3.77	+0.44
V781 Tau	0.3449	0.58	0.05	8.55	8.68	0.41	0.27	66.5	12.3	1.4	0.25	3.84	+0.08
W UMa	0.3336	0.62	0.00	7.76	7.85	0.49	0.10	86.0	20.2	1.1	0.12	4.29	+0.18
AW UMa	0.4387	0.35	0.00	6.84	6.91	0.07	0.65	79.1	15.1	0.9	0.13	2.73	-0.03
GR Vir	0.3470	0.57	0.00	7.80	7.93	...	...	...	18.8	1.2	0.14	4.17	+0.29

Table 2. Calibration Coefficients of CAL5

	$a_{P(BV)}$	$a_{BV}$	$a_0(BV)$
Average	−4.44	+3.02	+0.12
Median	−4.42	+3.08	+0.10
−1 $\sigma$ from median	−0.81	−0.70	−0.23
+1 $\sigma$ from median	+0.75	+0.51	+0.13

Table 3. Influence of a third parameter on the luminosity (in magnitudes per unit value)

Parameter	$q$		$f$		$i$	
	zero-point	slope	zero-point	slope	zero-point	slope
Average	−0.014	+0.05	+0.037	−0.05	−0.35	+0.0048
Median	−0.013	+0.04	+0.040	−0.06	−0.39	+0.0053
−1 $\sigma$ from median	−0.062	−0.21	−0.051	−0.11	−0.19	−0.0041
+1 $\sigma$ from median	+0.061	+0.21	+0.050	+0.15	+0.30	+0.0027